J4.9

VALIDATION OF A DATA ASSIMILATION TECHNIQUE FOR AN URBAN WIND MODEL

T.M. Booth and E. R. Pardyjak
University of Utah

1. INTRODUCTION

The QUIC (Quick Urban & Industrial Complex) dispersion modeling system has been developed to calculate wind and concentration fields in cities with buildings explicitly resolved (Pardyjak and Brown 2001; Williams et al. 2002). To improve the fast response 3D diagnostic urban wind model (QUIC-URB), a new data assimilation initialization scheme has been developed. The original QUIC-URB code initialized the flow field with horizontally uniform velocities based on wind speed and wind direction information obtained from a single sensor upwind of an urban area, but previous urban studies have shown that cities are often subject to large scale spatially varying inflows (e.g., Allwine et al. 2002). To attempt to account for this spatial heterogeneity, a simple Quasi-3D Barnes Objective Map Analysis Scheme (a Gaussian weighted-averaging technique) which initializes the flow field based on multiple sensors and soundings located around the urban area has been implemented. This wind field is then modified by QUIC-URB's empirical building flow parameterizations to model the flow around the individual buildings. The final flow field is then solved for by ensuring mass conservation.

This work is the first validation of the multi-sensor data assimilation QUIC-URB model. QUIC-URB mean 3D velocities are compared to the results of a FLUENT k-ε solution of the same urban environment. Individual vertical velocity profiles at various strategic locations around the urban area were extracted from the FLUENT data set to simulate soundings around an actual urban environment. These velocity profiles were then used as input parameters for QUIC-URB's new initialization scheme. After applying QUIC-URB's building parameterizations and enforcing mass conservation, the final wind fields from QUIC-URB and FLUENT were quantitatively compared. This comparison illuminated areas of deficiencies in the data assimilation model that are being used to improve the model.

2. QUASI-3D BARNES OBJECTIVE MAP ANALYSIS DESCRIPTION

The Quasi-3D Barnes map analysis is based on the 2D technique of Koch et al. (1983). The scheme begins by approximating a vertical velocity profile for every sensor data entered. The vertical velocity profiles are approximated by either a logarithmic function, exponential function or user data input profiles. An example is shown in Fig. 1 where the vectors represent the sensor data and the lines represent the approximated vertical velocity profiles at each sensor location.

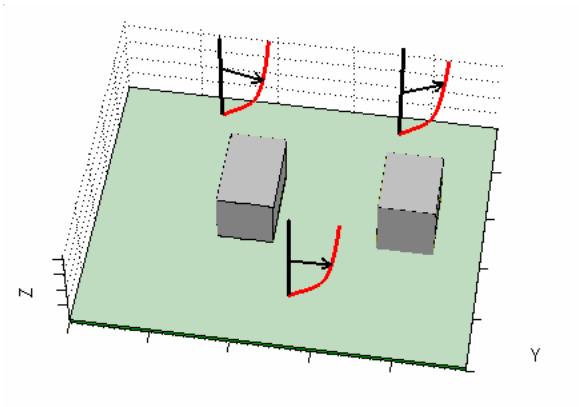

Figure 1: Example of an approximated vertical velocity profiles at each sensor data point.

To represent a Quasi - 3 dimensional flow field a horizontally planar flow field as shown in Fig. 2 is calculated at every grid cell height up to the full height of the computational domain.

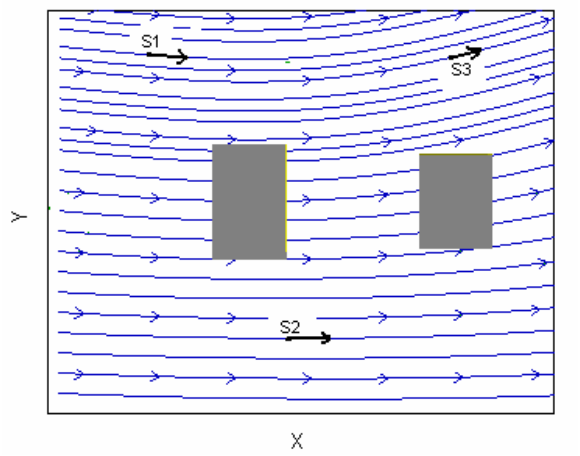

Figure 2: Example of a horizontal plane using the 2-D Barnes objective mapping technique.

The two dimensional Barnes objective map analysis scheme (details discussed later) calculates the 2D horizontally planar flow field at each grid cell height using the approximated values previously calculated. The resulting flow field is comprised of 2D horizontally planar flow fields "stacked-up" on top of each other as shown in Fig. 3.

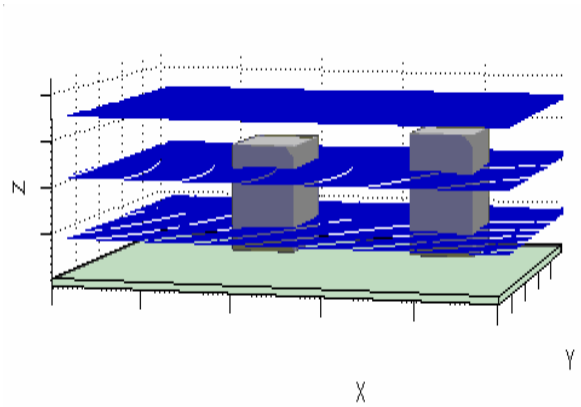

Figure 3: 2-D horizontal planar flow calculated for each grid cell height "stacked-up" to represent a quasi-3D flow.

3. 2D BARNES OBJECTIVE MAP ANALYSIS SCHEME

The Barnes objective map analysis scheme investigated here is based on the 2 dimensional interactive Barnes objective map analysis scheme for use with satellite and conventional data developed by Koch, DesJardins, and Kocin (1983). This model produces a Gaussian weighted average w_m of the form:

$$w_m = \exp\left(\frac{-r_m^{\,2}}{k}\right), \qquad (3)$$

where r_m is the distance between the computational grid point and the location of the sensor data point $u_{sensor}(x, y)$, and k is the weight parameter which determines the shape of the filter response function. For more details about the shape of the filter response function see Koch (1983).

The analysis scheme starts out by calculating a computational data spacing length. The computed data spacing length Δn is calculated by the average distance between each sensor data point $u_{sensor}(x, y)$ and its nearest neighbor. The weight parameter k_o for the first of the two computational iterations is then calculated from Δn by the following equation given by Koch et al. (1983).

$$k_o = 5.052\left(\frac{2\Delta n}{\pi}\right)^2 \qquad (4)$$

The first computational iteration calculates the weighted average at each grid cell location using k_o in Eq. 3 which produces an initial velocity field $u_o(x, y)$ from:

$$u_o(x, y) = \frac{\sum_{n=1}^{M} w_m u_{sensor}(x, y)}{\sum_{n=1}^{M} w_m}, \qquad (5)$$

where $u_{sensor}(x, y)$ is the velocity at each sensor location and m is the number of sensor data points located around the urban area. A new value $u_{\text{int}}(x, y)$ at each sensor location is linearly interpolated from the initial velocity field $u_o(x, y)$. The second computational iteration calculates the weighted average at each grid cell location using a new weight parameter k_1 for Eq. 3 given by

$$k_1 = k_o \gamma, \qquad (6)$$

where γ is the numerical convergence parameter that takes on values in the range 0.2 < γ < 1. With this convergence parameter the minimum error between the sensor data $u_{sensor}(x,y)$ and the final calculated velocity field $u_f(x,y)$ is given by γ=0.2 and the maximum error is given by γ=1. A constant γ value of 0.2 was used for this current model. This parameter will be the focus of future research.

The final velocity field $u_f(x,y)$ is calculated using the difference between the sensor data $u_{sensor}(x,y)$ and the new interpolated values $u_{\text{int}}(x,y)$ using the following expression:

$$u_f(x,y) = \frac{\sum_{n=1}^{M} w_m \left(u_{sensor}(x,y) - u_{\text{int}}(x,y)\right)}{\sum_{n=1}^{M} w_m} \quad (7)$$

4. DESCRIPTION OF THE TEST CASES

The urban environment chosen to be modeled in FLUENT and QUIC was similar to the Mock Urban Setting Test (MUST) array (Yee and Biltoft 2003). This urban environment was chosen since there is a plethora of field experiment data associated with it. In addition, it has already been carefully simulated by other researchers (Cameli et al. 2005) providing a standard to compare against. In the MUST experiment, a regular array of shipping containers was used to model buildings. The FLUENT model kept the same configuration, size and spacing of the shipping containers used in the MUST experiment, however the size of the array was reduced from the original MUST size of 11X12 containers to a 7X6 array of containers to save computational resources. A schematic of the 7X6 array is shown in Fig. 4. Figure's 5 and 6 show the spacing between the containers and the size of the containers respectively.

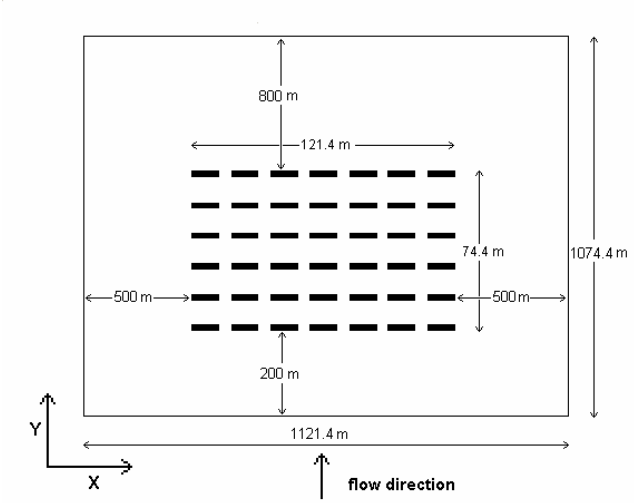

Figure 4: Schematic of the MUST array as implemented in FLUENT.

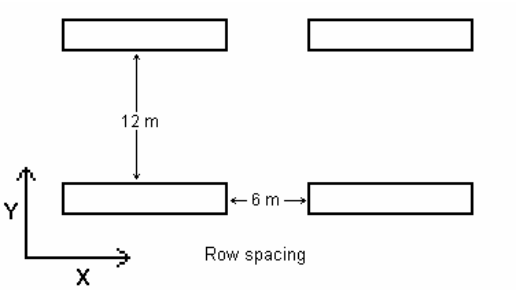

Figure 5: Row and column spacing used FLUENT simulations (QUIC used a column spacing of 6.1 m. as discussed later).

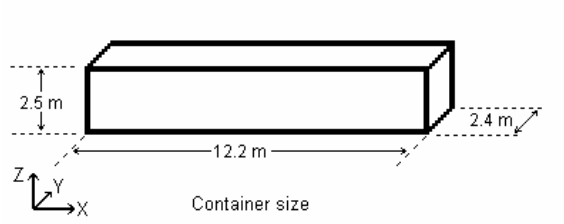

Figure 6: Shipping container dimensions modeled in the QUIC and FLUENT simulations.

The containers were each composed of elements with uniform mesh size. The containers were resolved into 5 elements in the y-direction, 5 elements in the z-direction, and 15 elements in the x-direction. The horizontal and vertical spacing between the containers also had uniform mesh sizes which resolved the rows into 15 elements wide and the columns into 10 elements wide. The domain outside of the container array had exponential spacing which

grew in size the farther away from the array. A view of this mesh is shown in Fig. 7.

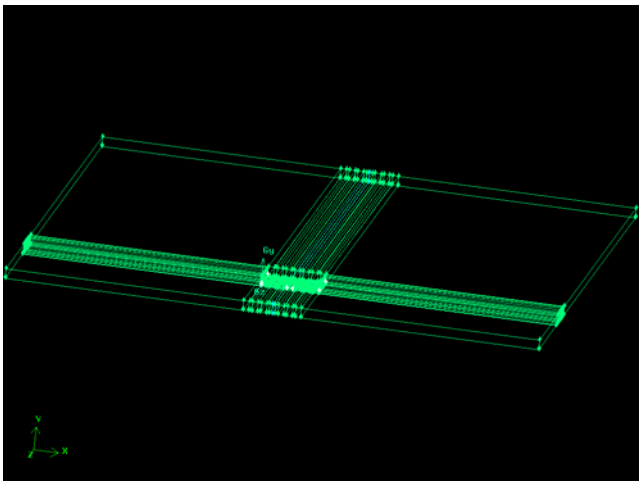

Figure 7: Mesh used in the FLUENT simulations of the MUST array.

The FLUENT model used was the standard *k-*ε turbulence model with default constants along with the SIMPLE pressure solver. To match the capabilities of QUIC-URB, the flow was modeled as isothermal and incompressible. The continuity and momentum equations were iterated until a convergence of criteria of 10^{-4} was met.

The boundary condition at the inlet was a simple power-law velocity profile with an exponent of 0.41, a reference velocity of 4 m/s and a reference height of 10 meters. The boundary conditions for the exit and the two sides were pressure outlets. The top face of the boundary was specified as a moving wall. A plot of the output velocity vector field is shown in figure 8.

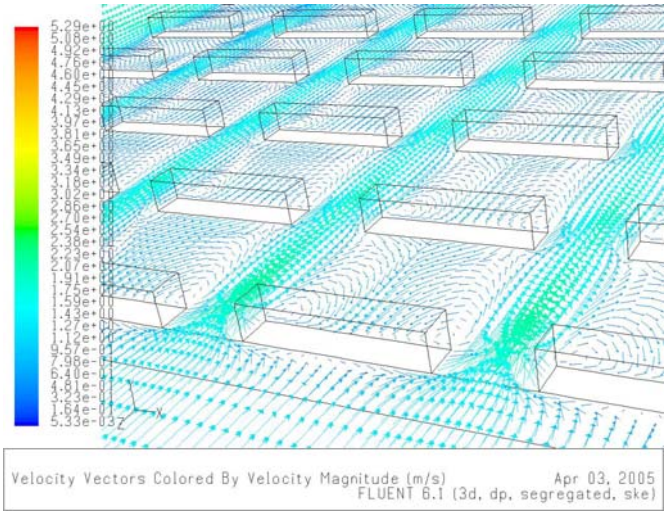

Figure 8: A sample vector field from the MUST FLUENT simulations at the lowest height level.

The urban environment used in the FLUENT model was duplicated in QUIC-URB. The size of the domain was reduced to an overall size shown in Fig. 9 to reduce the computational time.

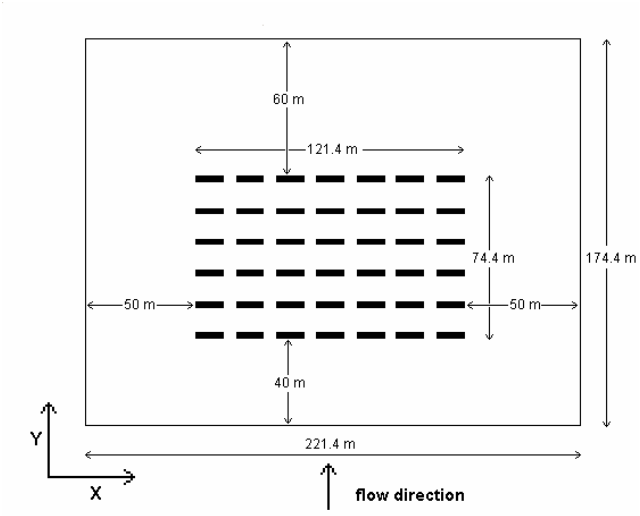

Figure 9: Schematic of the MUST array as implemented in QUIC-URB.

Due to the grid generating restrictions of QUIC-URB, it was not possible to recreate the exact mesh used with the FLUENT model, but it was matched as closely as possible. The grid has to be uniform in each direction (i.e. there can not be telescoping spacing like that used in FLUENT). The grid element sizes were set as follows:
dx = 0.7625 meters;
dy = 0.6 meters;

dz = 0.625 meters.

It was not possible to recreate the exact MUST array with these uniform grid sizes. With a dx grid size of 0.7625 the containers can be resolved into 16 elements wide, but the container spacing in that direction could not be resolved to 6 m. Instead the spacing had to be 6.1 m, which is 8 elements wide. This inconsistency affects the comparison of the FLUENT model to the QUIC model a great deal when the error of velocity fields were plotted as a contour. A contour plot of the true error and true % relative error is shown in the results and discussion section. However, this inconsistency is minor when viewing a horizontal velocity profile of the sets of data. One can see a minor shift in the QUIC data set, but it is still evident that the solutions are similar.

Three QUIC-URB cases were run to investigate the effects of assimilating data from various sensors throughout the modeled domain. In particular, the effect of the spatial locations of specific sensors was investigated. To do this, data from the FLUENT calculations were used as synthetic "sensor" data to drive the QUIC simulations. A schematic of the sensor placement in QUIC is shown in Fig. 10.

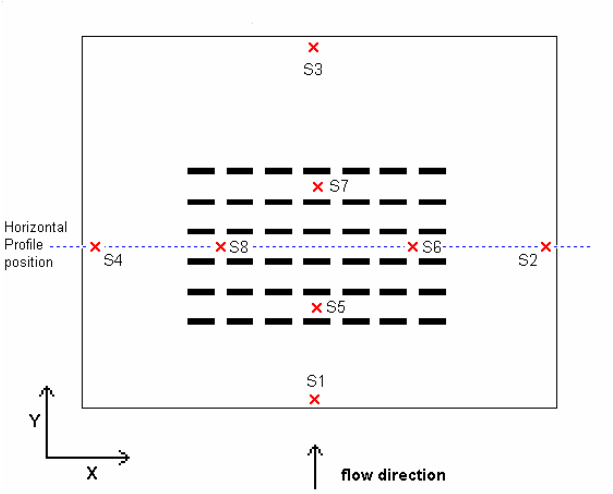

Figure 10: Schematic indicating the locations of the sensors used in the data assimilation scheme. Also shown is the plane used for horizontal velocity profile comparisons.

Each sensor is simply a vertical velocity profile extraction from the previously run MUST FLUENT model. The extracted vertical velocity profiles are shown in figures 11 & 12. Figure 11 shows the profiles that were located around the outside of the container array. Figure 12 shows the profiles extracted from inside the container array. These profiles show what was extracted from the MUST FLUENT model, but only the data points above the height of the containers (z>2.5) were used as input into QUIC. This was done to simulate real atmospheric sounding input into QUIC. Since the data assimilation algorithm is not designed to handle the type of complex flow associated with flow around buildings, within the building array QUIC-URB standard algorithms were used.

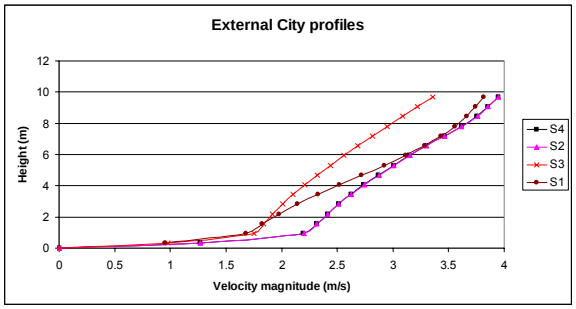

Figure 11: External city input velocity profiles (FLUENT output).

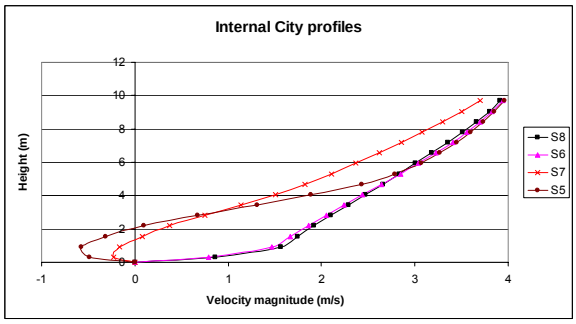

Figure 12: Internal city input velocity profile (FLUENT output).

In the first test case, only one upwind profile (S1) was used as input. This simulates the standard QUIC-URB model. The second case used 4 profiles located outside of the container array (S1, S2, S3, S4) to initialize the flow field. The last case utilized all 8 profiles to initialize the flow field.

Each case was executed using the same QUIC-URB model parameters given here:

Rooftop flag	=	1 – Logarithmic
Upwind Cavity flag	=	2 – MVP
Street Canyon flag	=	1 – Röckle

5. RESULTS AND DISCUSSION

Since the FLUENT model had a different mesh than the uniform mesh create by QUIC, a linear interpolation scheme was used to interpolate the FLUENT data onto the QUIC grid. This made it possible to assimilate the FLUENT profiles into QUIC and to compare data at the same nodes for the FLUENT and QUIC computations.

As briefly discussed earlier, the best way to view the error between the FLUENT and the QUIC model is a side by side comparison of velocity profiles as opposed to error contours. However, there is useful information in full plane error contours that should not be left out. Figure's 13 through 18 show comparisons of vertical velocity profiles at each of the "sensor" locations between the FLUENT model and the 3 different QUIC cases. Profiles at S4 and S8 were left out since they were identical to the profiles at S2 and S6 due to the symmetry of the problem.

Figure 13 shows that all but the 8 sensor case of QUIC agree very well. The error in the case of the 8 sensor array is inherent to the Barnes Objective mapping scheme. As discussed earlier, in order to converge on a solution within two iterations the input profiles are "relaxed" to better fit the overall average of data. The 8 sensor case at location S1 is relaxed since there is another profile at S5 which is close to the S1 location and has a larger velocity deficit region near the ground. The other cases do not experience this "relaxation" as much.

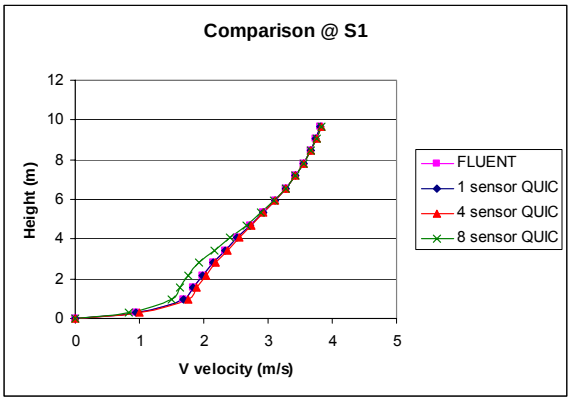

Figure 13: Streamwise velocity profile comparisons of FLUENT & QUIC at location S1.

Figure 14 shows a shortcoming of the single sensor case. The single sensor case initializes the whole domain with horizontally homogenous velocities, so this does not allow for the development of the boundary layer in the streamwise direction.

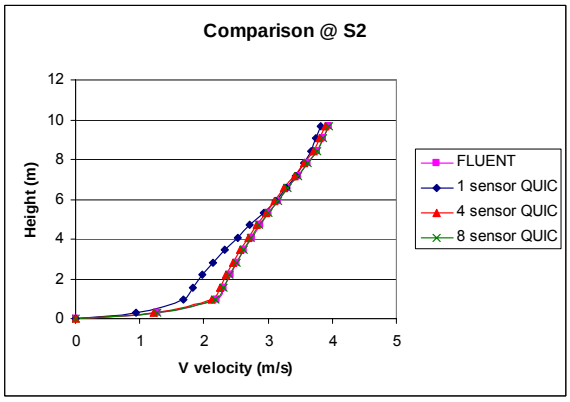

Figure 14: Streamwise velocity profile comparisons of FLUENT & QUIC at location S2.

Figure 15 shows another shortcoming of the single sensor QUIC calculation. Since this sensor is in the wake of the building array, the upper half of the profile should show signs of the velocity deficit stemming from the upwind container array. However, since QUIC does not solve an explicit equation for the diffusion of momentum, there is an under prediction of this deficit without the assimilated data.

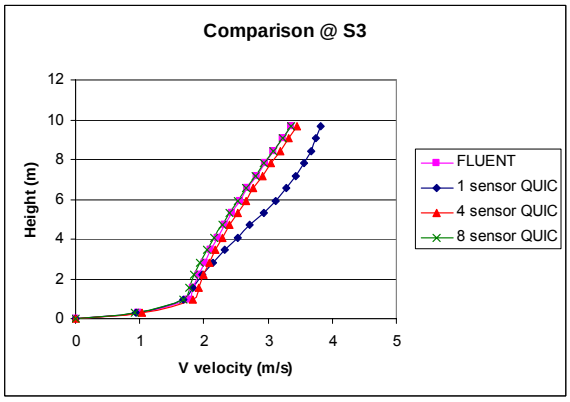

Figure 15: Streamwise velocity profile comparisons of FLUENT & QUIC at location S3

Figures 16 through 18 show the enhanced accuracy of placing sensors above the container array. These input profiles help to more accurately model the velocity deficit produced by the container array above the containers.

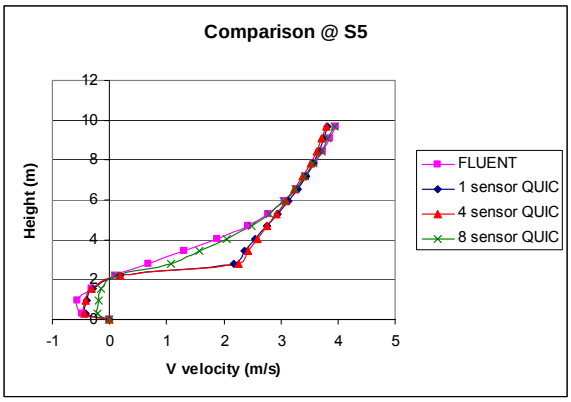

Figure 16: Streamwise velocity profile comparisons of FLUENT & QUIC at location S5

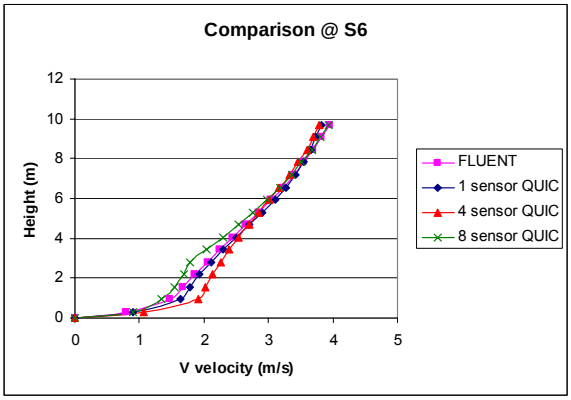

Figure 17: Streamwise velocity profile comparisons of FLUENT & QUIC at location at S6

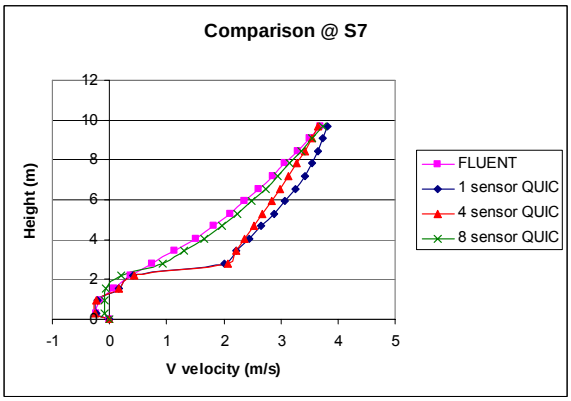

Figure 18: Streamwise velocity profile comparisons of FLUENT & QUIC at location S7

Figure's 19-21 show a horizontal velocity profile comparison between FLUENT and the three QUIC cases. This velocity profile was extracted from the data at 3 different heights at the location shown in Fig. 10. The three heights selected give a overall view of the accuracy of the 3 different QUIC cases. The first profile height is at mid-container height (z=1.56 m), with the second profile height just over the top of the containers (z=2.81 m) and the third profile height was at 2 times the containers height (z=5.31 m).

From Fig. 19, it is clear that the single sensor QUIC case does not have the increase in velocity around the sides of the container array that it should have. The error inside the container array is greater for the 8 sensor case than the 4 sensor case and even greater still than the single sensor case. This is largely due to the building parameterizations in QUIC. The building parameterizations do not include any forced street channeling. Street channeling is the accelerated flow along the streets due to a build up of pressure along the front of the buildings. However, this topic is for future work. The 8 sensor QUIC case does a good job in showing the velocity deficit region in the container array if street channeling was not evident. The velocities in the streets of the 8 sensor case are about the average of the velocities in the streets and behind the buildings in the FLUENT model.

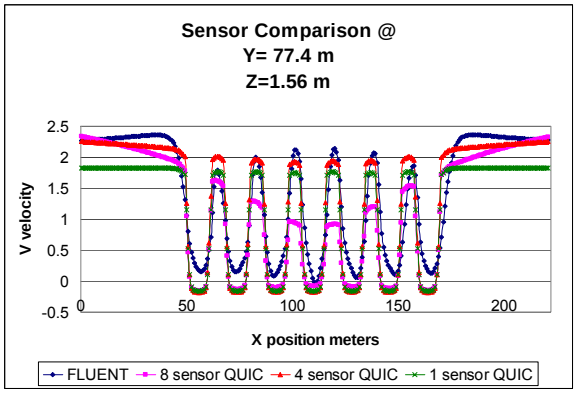

Figure 19: Horizontal velocity profiles of streamwise velocities from FLUENT and QUIC

Figure 20 shows the horizontal velocity profiles at the tops of the buildings. None of the QUIC cases show the same pattern as the FLUENT model. This is a shortcoming of the building top parameterizations of QUIC. Ignoring this shortcoming, the 8 sensor case does the best job in showing a velocity deficit region above the containers. However, it does appear to be slightly over predicting the velocity deficit region here.

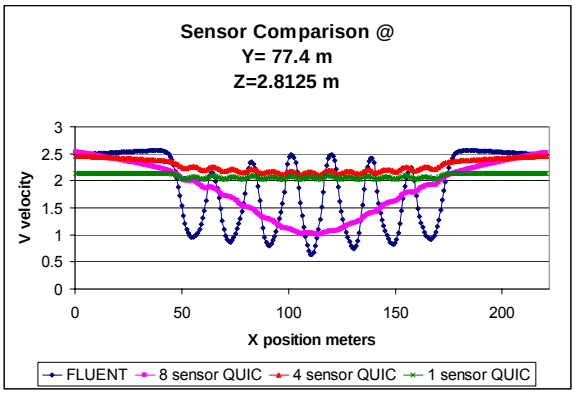

Figure 20: Horizontal velocity profiles of streamwise velocities from FLUENT and QUIC.

Figure 21 shows the comparisons of the horizontal velocity profiles at 2 times the height of the containers. The 8 sensor case does a better job at giving an average velocity than shown in the previous figure.

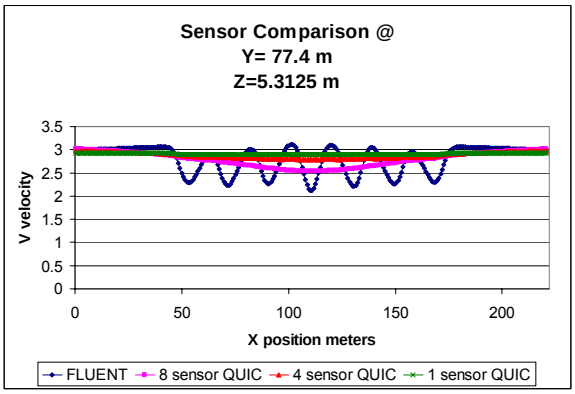

Figure 21: Horizontal velocity profiles of streamwise velocities from FLUENT and QUIC.

The next figures are error contours of the true error between the FLUENT model and the three different QUIC cases. Here, true error is defined by the difference between the streamwise velocities (i.e., True Error = Fluent – QUIC).

In Figs. 22-24 it is apparent that the single sensor case does not show the development of the boundary layer outside of the container array. Also, it should be noted that the majority of the error in these plots next to the buildings is due to the misalignment of the two separate grids as discussed in section 4. The first column of containers on the left in QUIC are correctly aligned with the FLUENT model, but the column spacing in QUIC is 6.1 meters as opposed to the 6 meter column spacing in FLUENT. This is why the error next to the columns of containers is growing as you move to the right of the array. To fix this problem, an element size of 0.2 meters is needed. Unfortunately, compared to the current 0.7625 meter elements size this would require a huge increase in computational resources.

Figures 24 & 27 shows the areas in red where there is street channel flow that is not properly being parameterized by QUIC.
Figure 30 shows that the 8 sensor case has the least amount of error around the array, but it still has some residual error from the street channel flow error from QUIC.

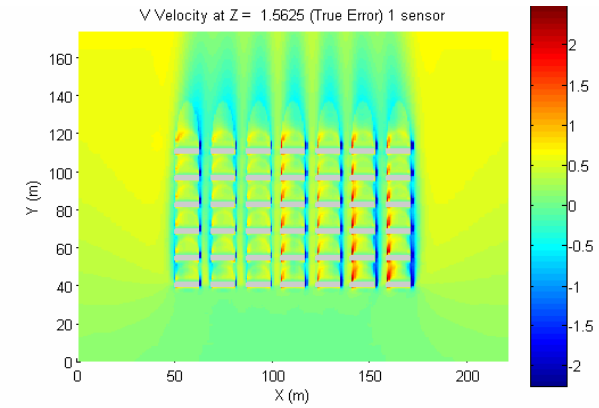

Figure 22: Contour plot of the True Error between the streamwise velocity of the FLUENT model and the 1 sensor QUIC model at z=1.5625 m.

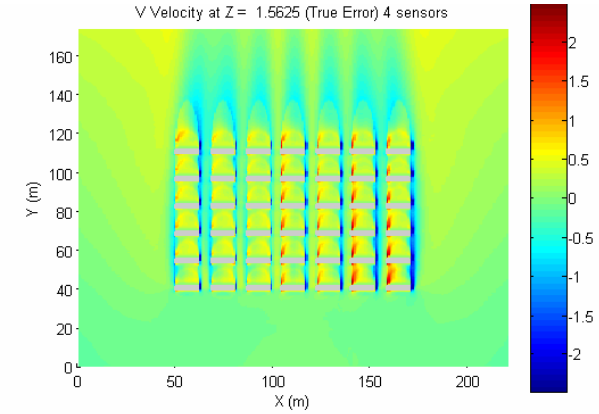

Figure 23: Contour plot of the True Error between the streamwise velocity of the FLUENT model and the 4 sensor QUIC model at z=1.5625 m.

.

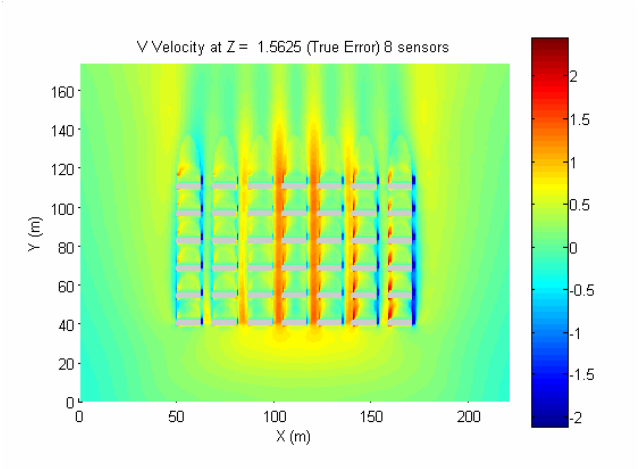

Figure 24: Contour plot of the True Error between the streamwise velocity of the FLUENT model and the 8 sensor QUIC model at z=1.5625 m

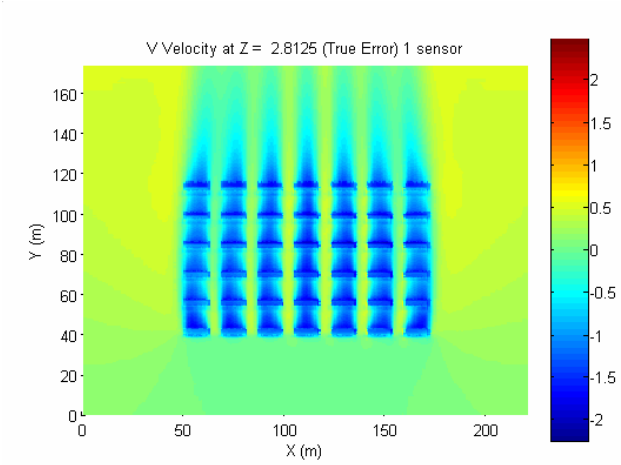

Figure 25: Contour plot of the True Error between the streamwise velocity of the FLUENT model and the 1 sensor QUIC model at z=2.8125 m.

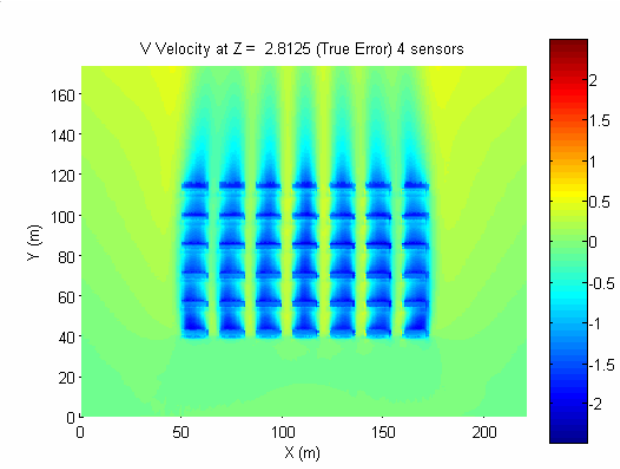

Figure 26: Contour plot of the True Error between the streamwise velocity of the FLUENT model and the 4 sensor QUIC model at z=2.8125 m.

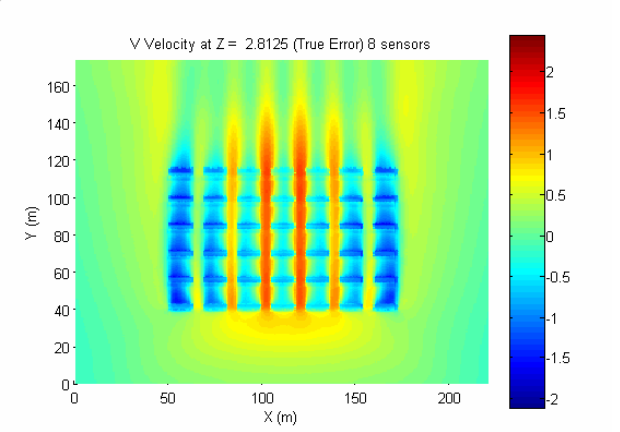

Figure 27: Contour plot of the True Error between the streamwise velocity of the FLUENT model and the 8 sensor QUIC model at z=2.8125 m.

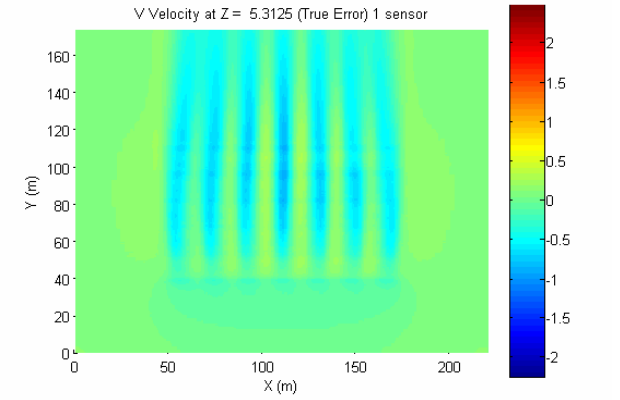

Figure 28: Contour plot of the True Error between the streamwise velocity of the FLUENT model and the 1 sensor QUIC model at z=5.3125 m.

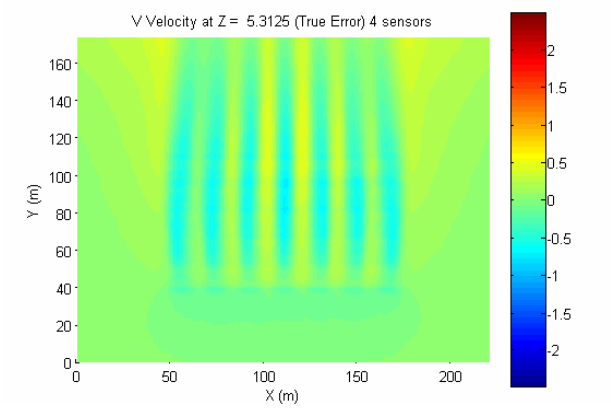

Figure 29: Contour plot of the True Error between the streamwise velocity of the FLUENT model and the 4 sensor QUIC model at z=5.3125 m.

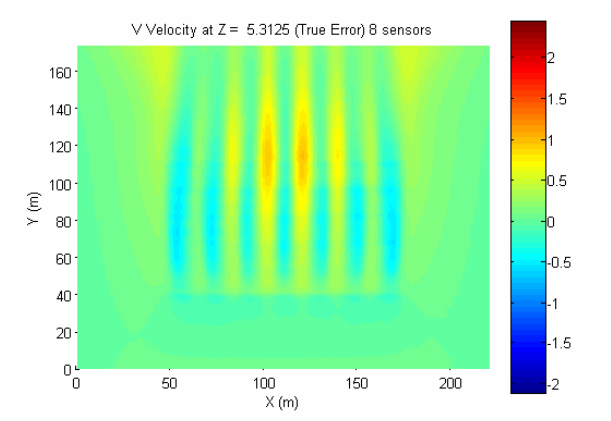

Figure 30: Contour plot of the True Error between the streamwise velocity of the FLUENT model and the 8 sensor QUIC model at z=5.3125 m.

6. SUMMARY

This preliminary work seems to indicate that utilizing a simple quasi-3D data assimilation technique to ingest soundings from multiple locations is more accurate than the standard single sensor method typically used to initialize QUIC simulations. However, the theory of "the more sensors, the better the result" is in debate. The 8 sensor case showed more promise than the 4 sensor case, but it still had larger error. The "smart" placement of sensors would seem to result in a more accurate solution. Obviously, if the whole domain was filled with sensor readings the QUIC results should match the synthetic data. Unfortunately, this is not the case in the real world. Given a limited set of sensors options, it is necessary to place them in the positions that compliment each other and the building parameterizations in QUIC to produce the most accurate results. Clearly, additional work is needed in this area.

Further research topics might include the use of the street channel measurements to improve a street channeling parameterization, ideal placements of sensors throughout cities and possible localization algorithms for measurements well below building heights.

5. REFERENCES

Allwine, K.J., Shinn, J.H., Steit, G.E., Clawson, K.L., and M.J. Brown, 2002: Overview of URBAN (2000) A multiscale field study of dispersion through an urban environment. *Bulletin of the American Meteorological Society*, **83**, 521-536.

Camelli, F., R. Lohner, and S. Hanna (2005) VLES study of MUST experiment, AIAA-2005-1279, *43rd AIAA Aerospace Sciences Meeting and Exhibit*, Reno, Nevada, Jan. 10-13.

Koch, S. E., M. DesJardins and P.J. Kocin (1983) An interactive Barnes objective map analysis scheme for use with satellite and conventional data. *J. Climate and Appl. Meteor.*, **22**, 1487-1502.

Pardyjak, E.R. and M.J. Brown (2001) Evaluation of a fast-response urban wind model: comparison to single building wind-tunnel data. *Proceedings of the 3rd International Symposium on Environmental Hydraulics*. D. Boyer and R. Rankin (Eds.), Tempe, AZ.

Williams, M.D., M. J. Brown and E. R. Pardyjak, (2002) Development and testing of a dispersion model for flow around buildings, *4th AMS Symp. Urban Env.*, Norfolk, VA.

Yee, E. and C. A. Biltoft (2003) Concentration fluctuation measurements in a plume dispersing through a regular array of obstacles, Boundary-Layer Meteorology, **111**, 363 - 415